3.1 Bericht Teilprojekt 2

3.1.1 Titel / Title

Theoretische Untersuchungen der spektroskopischen Eigenschaften von Silizium-Nanoteilchen

Theoretical investigations of the spectroscopic properties of silicon nanocrystals

3.1.2 Berichtszeitraum / reported period

01.07.2003 - 30.11.2006

3.1.3 Projektleiter / principle investigator

Scholz, Reinhard, Dr., Oberassistent
Technische Universität Chemnitz (bis Dezember 2006)
Technische Universität München (seit März 2006)

Schreiber, Michael, Prof. Dr.
Technische Universität Chemnitz

3.2 Zusammenfassung / Abstract

3.2.1 Wortlaut des Antrags / abstract of the proposal

Verschiedene Ansätze zur theoretischen Behandlung der optischen Eigenschaften von interstellaren Staubteilchen sollen in diesem Teilprojekt am Beispiel von Silizium-Nanokristallen entwickelt werden. Von der Anwendung empirischer Tight-Binding-Verfahren (ETB) und Dichtefunktional-basierter Tight-Binding-Methoden (DFTB) erwarten wir ein mikroskopisches Verständnis der spektroskopischen Eigenschaften dieser Nanoteilchen. Dafür ist die Berechnung der relaxierten Geometrien der Nanokristalle mit bzw. ohne Passivierung der Oberfläche mit Wasserstoff oder Sauerstoff vonnöten. Die optischen Anregungen sollen mit zeitabhängiger Dichtefunktionaltheorie (TD-DFT) und empirischem Tight-Binding untersucht werden. Eine von einer umgebenden Oxidschicht hervorgerufene Verspannung des Si-Kerns eines solchen Nanoteilchens soll mit DFT-Verfahren berechnet werden. Die für die entsprechende Geometrie auftretenden Anregungsenergien sollen mit gemessenen Absorptions- und Photolumineszenz-Spektren verglichen werden. Für unvollständig passivierte Teilchen soll die Entstehung von Zuständen innerhalb der Bandlücke durch dangling bonds und Zustände an der Grenzfläche Silizium-Siliziumoxid sowie deren Einfluss auf die Photolumineszenz untersucht werden. Die dafür benötigten Veränderungen der Bindungsgeometrie im relaxierten angeregten Zustand sollen mit einer Verallgemeinerung des DFTB-Verfahrens auf elektronisch angeregte Zustände berechnet werden.

Different theoretical approaches for the investigation of the optical properties of interstellar dust shall be developed in the present project for the model system of nanocrystalline silicon. We want to obtain a microscopic understanding of the spectroscopic properties of these nanoparticles by applying empirical tight-binding (ETB) and density functional tight-binding (DFTB) techniques. This requires the computation of the relaxed geometries of the nanocrystals with and without hydrogen or oxygen passivation of the surface, and of the optical excitations with time-dependent density functional theory (TD-DFT) and empirical tight-binding. The strain induced by a surrounding silicon oxide layer on the crystalline core of the nanoparticle shall be computed on an atomistic level. The excitation energies calculated for the corresponding geometry shall be compared with the measured absorption and photoluminescence spectra. For incompletely passivated particles, the appearance of mid-gap states due to dangling bonds and to trap states at the interface between silicon and its oxide and their influence on the photoluminescence spectra shall be investigated. Changes of the bond geometry in the relaxed excited state of the nanoparticle shall be computed with extensions of the DFTB approach to optically excited electronic configurations.

3.2.2 Zusammenfassung des Berichts / abstract of the report

Durch die indirekte Bandstruktur von Silizium erfordert die impulserhaltende Photolumineszenz (PL) im Bulkmaterial die Absorption oder Emission eines Phonons. Weil die Quantisierung der elektronischen Zustände in passivierten Nanokristallen einer Ausschmierung der Wellenfunktion über einen größeren Bereich der Brillouin-Zone entspricht, ist die erforderliche Impulserhaltung in solchen Strukturen ohne Assistenz eines Phonons

möglich. Die erhöhte PL-Effizienz und die Ähnlichkeit der PL-Spektren mit den breiten Emissionsbanden aus dem interstellaren Raum (Extended Red Emission, ERE) hat zu dem Vorschlag geführt, dass nanokristallines Silizium der Träger der ERE sein könnte. Aus einem numerischen Blickwinkel sind solche Nanostrukturen mit mehreren Hundert Atomen sehr anspruchsvoll, so dass verschiedene komplementäre Methoden verfolgt worden sind, um ihre Geometrie und ihre spektroskopischen Eigenschaften zu untersuchen.

Eine der größten Herausforderungen ist die Bereitstellung von relaxierten Strukturmodellen für Siliziumkristalle, die an der Oberfläche oxidiert sind. Beim Start von einfachen Modellgeometrien, in denen ein Silizium-Nanokristall in eine Schale aus Siliziumoxid eingebettet ist, verhindert die thermische Stabilität aller Oxidphasen die Anwendung von simulierter thermischer Behandlung. Als Resultat solcher Molekulardynamik-Simulationen bei erhöhter Temperatur ergibt sich ein geschmolzener Siliziumkern in einer kaum modifizierten Oxidhülle, wobei dieser Kern bei anschließender Abkühlung amorph bleibt. Als Alternative wurde die Kollision von schnellen Sauerstoffatomen mit der Oberfläche eines kalten Siliziumkristalls untersucht. Im Prinzip ist dieses Verfahren vielversprechend, aber es kann nicht ausgeschlossen werden, dass die Endgeometrien von den kleinen Basisätzen im Dichtefunktional-Tight-Binding (DFTB) und von den statistischen Eigenschaften der Anfangs-geometrien und Kollisionsenergien beeinflusst werden.

Um einen Einfluss der Geometrieoptimierung auf die spektroskopischen Eigenschaften zu vermeiden, wurden letztere für wohldefinierte Modellcluster untersucht: wasserstoffpassivierte Siliziumkristalle mit tetraedrischer Symmetrie. Für wesentlich kleinere Systeme bis zu $Si_{99}H_{100}$ (Durchmesser $d \leq 1.5$ nm), die alle um ein zentrales Siliziumatom herum angeordnet sind, wurde die Geometrie des Grundzustands mit Dichtefunktionaltheorie (DFT) optimiert, die Geometrie im angeregten Zustand mit zeitabhängiger Dichtefunktionaltheorie (time-dependent density functional theory, TD-DFT).

Elektronische Anregungen bewirken eine Veränderung der Besetzungszahlen der beteiligten Orbitale und somit eine anisotrope Veränderung der elektronischen Ladungsdichte. Diese anisotrope Ladungsdichte verursacht eine verringerte Symmetrie der relaxierten angeregten Zustände im Vergleich zur Punktgruppe T_d im elektronischen Grundzustand. In der resultierenden tetragonalen Symmetrie ist die Entartung des höchsten besetzten Orbitals (HOMO) aufgehoben. Diese mit der Symmetrieerniedrigung einhergehende Aufspaltung ist als Jahn-Teller-Effekt bekannt und erfolgt im wesentlichen proportional zur Abweichung von der tetraedrischen Geometrie des Grundzustands. Die Projektion der Deformation im relaxierten angeregten Zustand auf die verschiedenen Symmetrien erlaubt die Zuordnung der entsprechenden Beiträge zur Stokes-Verschiebung. Für einige der untersuchten Systeme ist der Beitrag der Symmetrieerniedrigung zur Rotverschiebung der PL größer als der Einfluss symmetrieerhaltender Deformationen.

Due to its indirect band structure, photoluminescence (PL) from bulk silicon requires phonon-assisted emission processes. In Si nanostructures like oxidized nanocrystals, the quantization of the electronic states corresponds to a spreading of the electronic states over a large range of wave vectors, resulting in momentum conservation in PL without phonon emission. The improved PL efficiency and the similarity of the PL spectra of size-selected samples with the extended red emission (ERE) from interstellar space has led to the proposition that nanosized oxidized silicon particles might be a possible carrier of the ERE. From a computational point of view, such particles containing several hundred atoms are very demanding, suggesting a combination of complementary approaches for the investigation of the geometry in the electronic ground state and spectroscopic aspects.

One of the major challenges is the definition of suitable atomistic model geometries for crystalline silicon embedded in an oxide matrix without large strain. Starting from simple model geometries consisting of a crystalline Si grain inserted into a shell of silicon oxide, the thermal stability of the various oxide phases inhibits the use of simple schemes for simulated thermal annealing. The result of such molecular dynamics (MD) simulations at elevated temperatures is a molten Si core embedded into an oxide shell which is hardly modified, and after lowering the simulation temperature, the core remains amorphous. As an alternative, we have investigated the collisions of fast oxygen atoms colliding with crystalline Si grains held at a temperature below the melting point. In principle, this route was found to be more promising, with the drawback that even in approximate schemes like DFTB, the computation of well-passivated Si clusters becomes rather tedious. Moreover, the results are likely to be influenced by the properties of the non-converged basis sets used, and by assumptions related to the ensemble of starting configurations and collision energies.

In order to circumvent any uncontrolled influence of a partly relaxed geometry on the spectroscopic properties, we have started to investigate the latter for well-defined model clusters: Nearly spherical approximants of tetrahedral Si crystals, with all surface dangling bonds passivated by hydrogen. For much smaller systems up to $Si_{99}H_{100}$ (diameter $d \leq 1.5$ nm), model clusters centered around a silicon atom at the origin were optimized with DFT, and for the excited state with TD-DFT.

Optical excitation produces a change of the occupation numbers of the frontier orbitals, corresponding therefore to an anisotropic modification of the total charge density. In turn, this anisotropy defines a relaxed

excited state geometry of lower symmetry with respect to the tetrahedral point group T_d of the electronic ground state. In the resulting tetragonal symmetry, the degeneracy of the HOMO is lifted. The splitting is proportional to the tetragonal deformation, a phenomenon which can be understood as a pronounced Jahn-Teller effect. The projection of the deformations at the minima of the excited state potential surface onto the different symmetries allows for a discrimination of the respective contributions to the total Stokes shift. For selected systems, the influence of the Jahn-Teller effect on the Stokes shift can exceed the red shift related to a symmetry-conserving deformation in the relaxed excited state.

3.3 Ausgangsfragen, neuster Stand der Forschung / Initial goals, current status of the field

After the observation of intense red PL from porous silicon (Canham 1990), various experimental investigations have focused on a reproducible generation of size-selected silicon nanoparticles with different preparation techniques, ranging from gas phase synthesis (Schuppler 1995, Ehbrecht 1997) over growth in nanosize surfactant aggregates (Wilcoxon 1999) and annealing of non-stoichiometric silicon oxide (Takeoka 2000) to selective electrochemical etching (Belomoin 2002). From the dependence of the PL spectra on size, there is clear evidence for quantum confinement effects and a high PL efficiency (Ledoux 2002), features which however require a surface passivation with oxygen or hydrogen (Ledoux 2001).

Even 16 years after the discovery of PL from silicon nanostructures, we did not find any publication where a PL lineshape of a silicon nanocrystal was calculated from the geometries of its relaxed ground and excited states. Instead, several groups have investigated the vertical transition energies in the ground state geometry absorption of such systems with TD-DFT, but the deformation in the relaxed excited state and the resulting Stokes shift did not receive a lot of attention. Our investigation (Scholz 2006) extends previous calculations of the optical properties of H-passivated Si nanoparticles (Puzder 2003, Mitas 2001, Rao 2004, Tsolakidis 2005) towards a detailed analysis of the influence of different kinds of deformations on the Stokes shift. Contrary to previous studies of the Stokes shift for H-passivated Si_{29} (Sundholm 2004) and excited state relaxations in larger tetrahedral systems (Franceschetti 2003), deformations conserving the initial symmetry and deformations towards a lower symmetry are determined separately.

3.4 Angewandte Methoden / Applied methods

In order to reconcile a high precision with an affordable effort, we use the mixed functional B3LYP and a double-ζ basis throughout. All calculations are performed with the *turbomole 5.7* program package. The silicon clusters are constructed from nearly spherical approximants to the tetrahedral bulk lattice. The ground state of each cluster is optimized in the full tetrahedral point group T_d, whereas the T_d-symmetric deformation of the optically excited state and a symmetry lowering towards the subgroup D_{2d} are treated separately. At the present stage of the project, the deformations in the relaxed excited state have been determined for H-passivated Si clusters of a diameter of $d \leq 1.5$ nm, and the next step will be to project these deformations onto the vibrational eigenvectors of the ground state potential energy surface, resulting eventually in calculated PL lineshapes including the vibronic subbands.

In collaboration with TP 11, similar calculations have been applied to the vibronic bands observed in gas phase absorption spectra obtained on benzofluorene, see below.

3.5 Ergebnisse und ihre Bedeutung / Results and their importance

3.5.1 Silicon nanoparticles

In all nonlinear closed shell molecules, optical excitation results in a spontaneous symmetry breaking with respect the geometry of the ground state, a phenomenon known as the Jahn-Teller effect (Jahn 1937). Therefore, for a quantitative interpretation of absorption and PL, it is of utmost importance to determine the reduced symmetry at the minima of the excited state potential energy surface (PES).

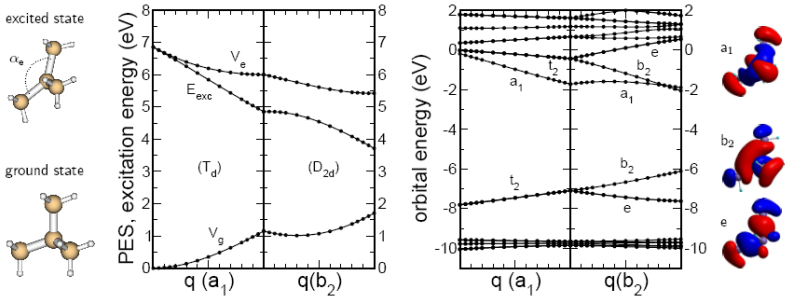

Fig. 1: Results of B3LYP/double-ζ calculations obtained forSi_5H_{12}. From left to right: Geometries in the D_{2d}-symmetric relaxed excited state (top) and in the T_d-symmetric electronic ground state (bottom); transition energies E_{exc} and potential energy surfaces of ground (V_g) and excited states (V_e) for the part $q(a_1)$ of the deformation in the relaxed excited state conserving the tetrahedral symmetry of the electronic ground state and for the subsequent tetragonal deformation $q(b_2)$ from T_d into a geometry with reduced D_{2d} symmetry; orbital energies for the deformation $q(a_1)$, and splitting of orbitals along the deformation $q(b_2)$; frontier orbitals in the relaxed excited state: a_1 (LUMO), b_2 (HOMO), and e (HOMO-1).

For the spherical approximants to a tetrahedral bulk lattice centered around a silicon atom investigated in the following, all dangling bonds at the surface are passivated with hydrogen atoms. For silane (SiH_4) and the molecules Si_5H_{12} and $Si_{17}H_{36}$, the terminal Si atoms have more than two hydrogen neighbours. As these systems are still too small to form closed six-membered Si rings, the dendrimer-like bond geometries remain rather flexible. In the electronic ground state of these systems, the t_2-symmetric HOMO is occupied by 6 electrons, resulting in an A_1-symmetric electronic configuration. After a dipole-allowed excitation to the a_1-symmetric LUMO, the symmetry of the electronic configuration is reduced to $(t_2)^5 a_1 = T_2$, inducing a distortion of the molecular geometry to tetragonal symmetry. Both the deformations conserving the tetrahedral point group T_d and subsequent D_{2d}-symmetric distortions give large reductions of the excitation energy, compare Figs. 1 and 2. The relaxed excited geometries of Si_5H_{12} and $Si_{17}H_{36}$ reveal strong deviations of the bond angle α_e around the central atom from a regular tetrahedron. This lowering of the symmetry results in a splitting of the threefold degenerate highest t_2 orbital into a HOMO transforming according to the b_2 representation in the subgroup $D_{2d} \subset T_d$ and a double degenerate orbital of e symmetry.

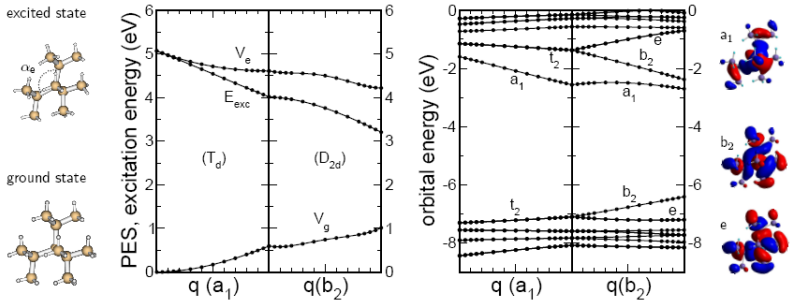

Fig. 2: As Fig. 1, but for $Si_{17}H_{36}$.

As the deformation responsible for the symmetry lowering consists mainly in a distortion of the bond angles between adjacent bonds around the central atom, only orbitals with a large contribution at this site are strongly influenced. More specifically, the highest occupied orbitals of t_2 symmetry are based on p orbitals on the central atom, splitting into a higher b_2 orbital with a node plane normal to the direction of the tetragonal compression of the tetrahedron, and a lower pair of e orbitals where the tetragonal axis is included in the node plane. The t_2 states above the LUMO consist mainly of p orbitals on the central atom, but in this case superimposed in an anti-bonding fashion with contributions localized around peripheral atoms. The a_1-symmetric LUMO is based on an s-symmetric orbital on the central site, surrounded by p-symmetric contributions from the peripheral Si atoms. It has a non-monotonous dependence on the deformation $q(b_2)$ in D_{2d}, so that the PES of the excited state results in a saddle point for $q(b_2) \rightarrow 0$. The curvature of the excited state

potential along this direction is an immediate consequence of this specific dependence of the energy of the a_1 orbital on the tetragonal deformation.

In Fig. 3 and Table I, we compare the influence of the tetrahedral and tetragonal parts of the deformation in the relaxed excited geometries of Si-H clusters on their respective excitation energies. Beyond $Si_{17}H_{36}$, all clusters have surface Si atoms bound into six-membered silicon rings, with the exception of $Si_{71}H_{84}$ where the surface is terminated by $–SiH_3$ end groups.

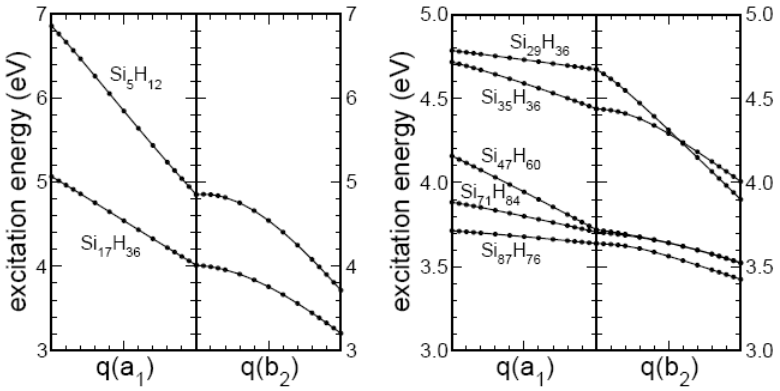

Fig. 3: Excitation energies of H-passivated silicon nanocrystals as a function of the tetrahedral part $q(a_1)$ and the tetragonal part $q(b_2)$ of the deformation in the relaxed excited state. Left: Si_5H_{12} and $Si_{17}H_{36}$, as annoted; right: $Si_{29}H_{36}$, $Si_{35}H_{36}$, $Si_{47}H_{60}$, $Si_{71}H_{84}$, and $Si_{87}H_{76}$.

For the small dendrimer-like molecules Si_5H_{12} and $Si_{17}H_{36}$, the tetrahedral $q(a_1)$ deformation induces a significant stretching of the bonds surrounding the central site, resulting in turn in a large Stokes shift exceeding 1 eV. The tetragonal $q(b_2)$ deformation, on the other hand, has a much smaller influence on the bond length, modifiying merely the angles between these bonds. The corresponding Jahn-Teller contribution to the Stokes shift is 1.1 eV (Si_5H_{12}) and 0.8 eV ($Si_{17}H_{36}$), remaining below the influence of the tetrahedral deformation for both molecules. In silane, the Stokes shift is even larger: 2.5 eV for the tetrahedral deformation $q(a_1)$, and 1.5 eV for the tetragonal distortion $q(b_2)$. Even though the larger Si nanocrystals are expected to be more rigid, they still experience a large red shift of the PL. Moreover, in $Si_{29}H_{36}$, $Si_{35}H_{36}$, $Si_{71}H_{84}$ and $Si_{87}H_{76}$, the Jahn-Teller contribution to the Stokes shift exceeds the influence of the tetrahedral deformation, whereas only in $Si_{47}H_{60}$, the tetrahedral deformation is dominant.

TABLE I: Geometric parameters of the optimized geometry of H-passivated Si clusters, calculated transition energies, and Stokes shift. d_g, d_e: bond length (Å) around the central atom in the electronic ground and excited states, respectively; α_e: angle (degrees) between bonds around central atom in the relaxed excited state. Where available, the calculated absorption energy E_{abs} is compared to experimental data, and the calculated values for the tetrahedral and tetragonal contributions to the Stokes shift ΔE are reported separately.

	SiH_4	Si_5H_{12}	$Si_{17}H_{36}$	$Si_{29}H_{36}$	$Si_{35}H_{36}$	$Si_{47}H_{60}$	$Si_{71}H_{84}$	$Si_{87}H_{76}$
$d_g(T_d)$	1.49	2.38	2.45	2.40	2.40	2.47	2.42	2.40
$d_e(T_d)$	1.73	2.70	2.68	2.40	2.43	2.59	2.46	2.43
$d_e(D_{2d})$	1.69	2.64	2.63	2.41	2.41	2.59	2.45	2.41
α_e	148.2	140.3	128.2	112.7	111.7	113.5	112.2	111.4
E_{abs}	10.44 (8.8[a])	6.85 (6.5[b])	5.07	4.79	4.72	4.16	3.88	3.71
$\Delta E(T_d)$	-2.54	-2.00	-1.05	-0.11	-0.28	-0.44	-0.18	-0.08
$\Delta E(D_{2d})$	-1.57	-1.14	-0.81	-0.77	-0.43	-0.20	-0.18	-0.21

a (Itoh 1986), *b* (Delley 1993)

3.5.2 Absorption spectra of benzofluorene

In collaboration with TP 11, we have investigated the lowest excitation of benzofluorene, $S_1 \leftarrow S_0$. Similar to previous DFT calculations based on the BLYP functional (Banisaukas 2004), our TD-DFT calculations based on B3LYP gave an inversion of the lowest two excitations: The strong $S_2 \leftarrow S_0$ transition measured at about E_{00}=32030 cm^{-1} (Banisaukas 2004) was found *below* the weak $S_1 \leftarrow S_0$ transition observed at E_{00}=29894 cm^{-1} (compare TP 11). For basis sets up to double-ζ, the lowest two excited state PES crossed

between the ground state geometry and the relaxed excited geometry of the PES in the electronic configuration S_1. Only a rather large triple-ζ basis gave PES of S_1 and S_2 which did not cross between the geometries of interest, compare Fig. 4.

Both excited PES have a modified curvature with respect to the ground state. This can be interpreted as a modification of the mechanical properties of the chemical bonds resulting from the excitation of an electron from an occupied bonding orbital to a virtual anti-bonding orbital.

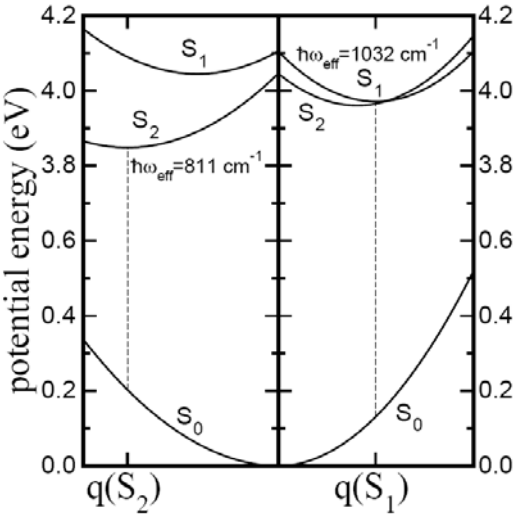

Fig. 4. Potential energy surfaces of the electronic configurations S_0, S_1 and S_2 of benzofluorene, as obtained in a TD-DFT calculation at the B3LYP/triple-ζ level. The electronic configurations are denoted according to the energetic ordering observed in the gas phase. The curvature on the PES of the excited states is given in terms of an effective vibrational mode $\hbar\omega_{\text{eff}}$ along the deformation between the relaxed geometries of the electronic ground state and the excited electronic configurations. With respect to the measured transition energies, the calculated origin band $E_{00}(S_1)$ is overestimated by about 0.30 eV, whereas the origin band $E_{00}(S_2)$ is underestimated by about -0.12 eV. This results in an inversion of the energetic ordering of the PES corresponding to S_1 and S_2.

TABLE II: Comparison of vibrational bands observed for the weak $S_1 \leftarrow S_0$ transition of benzofluorene with a TD-DFT calculation at the B3LYP/triple-ζ level. From left to right: observed transition energies; energies with respect to E_{00}; observed intensities, normalized to the transition at E_{00}+710 cm^{-1}; tentative assignment of the observations to vibrational modes calculated on the PES of S_0; ratio of mode frequencies deduced from the ratio of curvatures of the PES along the direction of the eigenvectors in the configuration S_0; Huang-Rhys factors obtained on the PES of S_0, normalized with respect to the intensity of the origin band E_{00}. The modes are assigned according to their ordering of the estimated frequencies $\hbar\omega(S_1)$.

E (cm^{-1})	***E*-*E*$_{00}$ (cm^{-1})**	**intensity**	**$\hbar\omega(S_0)$**	**$\hbar\omega(S_1)$/ $\hbar\omega(S_0)$**	**$S[\hbar\omega(S_0)]$**
29894.00	0	>> 1			**1.0**
30039.35	145.35	0.084	157	1.10	0.023
30192.50	298.5	0.055	314	1.04	0.028
30236.80	342.80	0.102	359	1.03	0.005
30448.50	554.50	0.115	590	1.02	0.080
30596.19	702.19	0.104	721	1.00	0.001
30603.91	709.91	**1.0**	764	0.93	0.095
30658.70	764.70	0.070	800	0.97	0.007
30701.50	807.50	0.049	?		
30711.40	817.40	0.094	847		0.026
30852.00	958.00	0.053	?		
30878.00	984.00	0.264	1036	0.99	0.027
31208.00	1314.00	0.106	1344	1.03	0.011
31230.20	1336.20	0.129	1599	0.90	0.032
31265.00	1371.00	0.138	1378	1.05	0.042
31269.00	1375.00	0.725	1637	0.89	0.080
			1400	1.05	0.049
31288.00	1394.00	0.235	1503	0.99	0.028
31359.20	1465.00	0.735	1464	1.01	0.062
			1503	0.99	0.028
			1632	0.92	0.020
			1608	0.95	0.054

From the measured intensities of the various vibronic sidebands, we can deduce an effective mode energy of 1058 cm^{-1} along the deformation between the relaxed geometries of the states S_0 and S_1, reproduced in the B3LYP/triple-ζ calculation within 3%. The projection of the deformation pattern at the minimum of the PES related to S_1 onto the vibrational eigenvectors determines the Huang-Rhys factor $S(\hbar\omega)$ of all vibrational modes of *a'* symmetry. These values for $S(\hbar\omega)$ give directly the ratio between the intensities of the first vibronic transition E_{01} of each mode with respect to the origin band E_{00}.

In the calculations performed till now, it turned out that the curvature of the S_1 PES along a vibrational eigenvector on the PES of S_0 can be strongly modified, compare Table II. Based on these large changes of the curvature, we suspect that the change in the electronic configuration will induce a substantial Dushinsky rotation between the two sets of vibrational eigenvectors. Therefore, the projection of the relaxed excited state deformation onto the vibrational eigenvectors on the PES of S_0 can only serve as a preliminary interpretation of the vibronic progression observed in absorption, and a more quantitative analysis would require the use of the eigenvectors on the upper PES corresponding to S_1. Such a projection scheme allowing for different eigenvectors on the PES corresponding to S_0 and S_1 would improve the vibrational frequencies, and it would significantly modify the assignment of the Huang-Rhys factors. At the present stage, the corresponding calculation of the vibration eigenvectors on the upper PES is under way.

3.6 Zusammenfassung und Ausblick / Summary and future

Mit DFT und TD-DFT wurden die Geometrien von H-passivierten Si-Kristallen bis zu einem Durchmesser von 1.5 nm im elektronischen Grundzustand und im symmetriegebrochenen angeregten Zustand optimiert. Für alle untersuchten Modellcluster wurde der Einfluss der tetragonalen und tetraedrischen Deformation auf die Stokes-Verschiebung einzeln bestimmt, so dass ein quantitativer Vergleich des Jahn-Teller-Effekts mit symmet-

rieerhaltenden Verformungen möglich war. In einigen der untersuchten Fälle war der Einfluss der Symmetrieerniedrigung auf die Rotverschiebung dominant.

Der nächste Schritt unserer Untersuchungen wird die Projektion der Deformationen auf die Vibrationseigenvektoren im elektronischen Grundzustands sein, so dass die vibronischen Progressionen in den PL-Spektren erstmals berechnet werden können. Von einem methodischen Standpunkt betrachtet ist die einzige benötigte Information der Huang-Rhys-Faktor jeder Vibrationsmode. Der einzige Unterschied zu einer quantitativen Analyse der vibronischen Banden in der Absorption ist die für die Projektion verwendete Potentialfläche: Absorption muss auf der angeregten Potentialfläche analysiert werden, PL auf der Fläche des elektronischen Grundzustands.

Für Benzofluoren wurde die Deformation in den relaxierten Geometrien der zwei niedrigsten angeregten Zustände ermittelt. Die Verteilung der stark ausgelenkten Moden im elektronischen Grundzustand auf verschiedene Frequenzbereiche entspricht im wesentlichen den in TP 11 beobachteten Absorptionslinien. Der nächste Schritt wird eine Berechnung der Vibrationsmoden im elektronisch angeregten Zustand sein, so dass die Dushinsky-Rotationen quantifiziert werden können. Darüber hinaus erwarten wir von einer Projektion der Verformung auf die Vibrationsmoden im elektronisch angeregten Zustand eine bessere Übereinstimmung mit den experimentell ermittelten Modenintensitäten.

Applying DFT and TD-DFT techniques to H-passivated silicon clusters in the size range up to a diameter of 1.5 nm, we have determined their geometries in the electronic ground state and at the minima of the excited state potential energy surface. In each case, tetrahedral and tetragonal deformations in the relaxed excited state were determined separately, allowing for a quantitative assignment of the influence of the Jahn-Teller effect on the Stokes shift. In specific cases, it was demonstrated that the energetic influence of a tetragonal distortion towards D_{2d} symmetry can exceed the Stokes shift resulting from a tetrahedral deformation alone.

A straightforward extension of the present work will be the projection of the deformation in the relaxed excited state of each Si nanocrystal on the vibrational eigenvectors of the ground state potential energy surface (Pouladsaz 2007). Presumably, this will result in the first calculation of the PL spectra of Si nanoparticles including the vibrational subbands. From a methodological point of view, such a calculation is directly based on the determination of the Huang-Rhys factors. The only difference with respect to an interpretation of the absorption spectra is the PES used in the projection scheme: Absorption has to be analysed on the PES of the excited state, PL on the PES of the ground state.

Concerning benzofluorene, we have calculated the elongation of the vibrational modes obtained on the PES of the electronic ground state in the relaxed excited geometry of the S_1 configuration. The main results were compatible with the gas phase spectra determined in TP 11, including the intensity distribution over regions with prominent modes. The next step will be a calculation of the vibrational modes in the PES of the excited state S_1, allowing a detailed assignment of Dushinsky rotations. We expect that a projection scheme based on the vibrational modes obtained on the excited PES will lead to an improved distribution of the intensities over the vibronic sidebands.

3.7 Literatur / References

Banisaukas, J., Szczepanski, J., Vala, M., and S. Hirata, *Vibrational and electronic absorption spectroscopy of 2,3-benzofluorene and its cation*, J. Phys. Chem. **A 108** (2004) 3713.

Belomoin G., Therrien J., Smith A., Rao S., Twesten R., Chaieb S., Nayfeh M. H., Wagner L., and Mitas L., *Observation of a magic discrete family of ultrabright Si nanoparticles*, Appl. Phys. Lett. **80** (2002) 841.

Canham L. T., *Silicon quantum wire array fabrication by electrochemical and chemical dissolution of wafers*, Appl. Phys. Lett. **57** (1990) 1046.

Ehbrecht M., Kohn B., Huisken F., Laguna M. A., and Paillard V., *Photoluminescence and resonant Raman spectra of silicon films produced by size-selected cluster beam deposition*, Phys. Rev. B **56** (1997) 6958.

Itoh U., Toyoshima Y., Onuki H., Washida N., and Ibuki T., *Vacuum ultraviolet absorption cross sections of SiH_4, GeH_4, Si_2H_6, and Si_3H_8*, J. Chem. Phys. **85** (1986) 4867.

Delley B. and Steigmeier E. F., *Quantum confinement in Si nanocrystals*, Phys. Rev. B 47 (1993) 1397.

Jahn H. A. and Teller E., *Stability of polyatomic molecules in degenerate electronic states. I. Orbital degeneracy*, Proc. Roy. Soc. **A 161** (1937) 220.

Ledoux G., Gong J., and Huisken F., *Effect of passivation and aging on the photoluminescence of silicon nanocrystals*, Appl. Phys. Lett. **79** (2001) 4028.

Ledoux G., Gong J., Huisken F., Guillois O., and Reynaud C., *Photoluminescence of size-separated silicon nanocrystals: Confirmation of quantum confinement*, Appl. Phys. Lett. **80** (2002) 4834.

Mitas L., Therrien J., Twesten R., Belomoin G., and Nayfeh M. H., *Effect of surface reconstruction on the structural prototypes of ultrasmall ultrabright Si_{29} nanoparticles*, Appl. Phys. Lett. **78** (2001)1918.

Puzder A., Williamson A. J., Reboredo F. A., and Galli G., *Structural Stability and Optical Properties of Nanomaterials with Reconstructed Surfaces*, Phys. Rev. Lett. **91** (2003) 157405.

Pouladsaz D., thesis: *Density functional studies of the spectroscopic properties of Si nanocrystals* (2007) in preparation.

Rao S., Sutin J., Clegg R., Gratton E., Nayfeh M. H., Habbal S., Tsolakidis A., and Martin R. M., Excited *states of tetrahedral single-core Si_{29} nanoparticles*, Phys. Rev. B **69** (2004) 205319.

Scholz R., Pouladsaz D. and Schreiber M., *Influence of the Jahn-Teller effect on absorption and photoluminescence spectra of Si nanocrystals*, phys. stat. sol. (c) **3** (2006) 3561.

Schuppler S., Friedman S. L., Marcus M. A., Adler D. L., Xie Y.-H., Chabal Y. J., Harris T. D., Brus L. E., Brown W. L., Chaban E. E., Szajowski P. F., Christman S. B., and Citrin P. H., *Size, shape, and composition of luminescent species in oxidized Si nanocrystals and H-passivated porous Si*, Phys. Rev. B **52** (1995) 4910.

Sundholm D., *Density functional studies of the luminescence of $Si_{29}H_{36}$*, Phys. Chem. Chem. Phys. **6** (2004) 2044.

Tsolakidis A. and Martin R. M., *Comparison of the optical response of hydrogen-passivated germanium and silicon clusters*, Phys. Rev. B **71** (2005) 125319.

Wilcoxon J. P., Samara G. A., and Provencio P. N., *Optical and electronic properties of Si nanoclusters synthesized in inverse micelles*, Phys. Rev. B **60** (1999) 2704.